Journal of Radioanalytical and Nuclear Chemistry (2024) 333:889–903
https://doi.org/10.1007/s10967-023-09251-2

Experimental study of long-term catalytic effect on hydrogen generation G value of water by gamma-ray irradiation and hydrogen diffusion analysis in Compacted Hulls and End-Piece waste

Junji Eto[1] · Masaki Kawai[1] · Masaaki Matsumoto[2] · Hirohisa Tanaka[3] · Ryutaro Hino[4] · Atsuhiko Terada[4] · Masashi Taniguchi[5] · Hitoshi Sugiyama[6]

Received: 9 May 2023 / Accepted: 1 November 2023 / Published online: 24 January 2024

Abstract
In this study, it was evaluated the long-term catalytic effect and catalyst poisoning effect of gamma-ray irradiation on zirconium molybdate hydrate in the presence of three-way catalysts. The results indicated that the three-way catalyst was effective in suppressing the increase in hydrogen concentration due to radiolysis without being affected by poisoning. In addition, hydrogen diffusion analysis of the compressed hull and endpiece waste shows that hydrogen flows well through the waste and is suppressed by a three-way catalyst located in the center of the waste headspace.

Keywords G value · Hydrogen generation · Hydrogen reduction catalyst · Hull and end-piece waste · Diffusion analysis

Introduction

In order to bury low-level radioactive waste in land disposal in Japan, it is required to be enclosed or solidified in a container so that radioactive materials do not leak easily and contamination does not spread out. It is known that in waste with a relatively high radiation dose rate, water left in the container is radiologically decomposed in long-term exposure of radiation derived from the waste, to generate combustible gases such as hydrogen [1]. In order to ensure the integrity of the waste container during the storage period, the concentration of flammable gas, especially hydrogen gas, generated in the container shall be below the combustion limit. Therefore, it is essential to remove moisture by drying them or some other meanswhen sealing waste into a container[2]. The hulls (shearing pieces of fuel cladding) and end pieces (end parts of fuel assemblies) generated by the operation of the reprocessing plant are planned to be removed by drying and be compressed, and then transferred into stainless steel containers with lids to be welded because of the relatively high radiation dose rate.

Zirconium molybdate hydrate ($Zr(OH)_2Mo_2O_7(H_2O)_2$, ZMH) produced by the reaction of molybdenum and zirconium adheres to the hull in the dissolution process of the reprocessing plant. Since ZMH has hygroscopicity characteristics and hydrogen is generated in the container by radiolysis due to re-hygroscopicity during drying and sealing processes, it is important to accurately evaluate the amount of hydrogen generated by radiolysis. In the case of a serious accident at a reprocessing plant, the pressure generated by a hydrogen explosion is important, and it is necessary to consider the possibility that the pressure generated when a hydrogen explosion occurs is more than twice the initial pressure. In order to prevent deflagration and detonation at the reprocessing plant, the hydrogen concentration in the deflagration area should be kept below the lower limit of 8 vol% [3].

✉ Junji Eto
junji_eto@mri.co.jp

1 Societal Safety and Industrial Innovation Division, Mitsubishi Research Institute, Inc., 10-3 Nagatacho 2-Chome Chiyoda-Ku, Tokyo 1008141, Japan

2 MRI Research Associates, Inc., 10-3 Nagatacho 2-Chome Chiyoda-Ku, Tokyo 1008141, Japan

3 Kwansei Gakuin University, 19-19 Tyayamachi Kita-Ku, Osaka 5300013, Japan

4 Japan Atomic Energy Agency, 765-1 Funaishikawa Tokai-Mura Naka-Gun, Ibaraki 3191184, Japan

5 Daihatsu Motor Co., 765-1 Funaishikawa Tokai-Mura Naka-Gun, Fukuoka 3191184, Japan

6 Utsunomiya University, 7-1-2 Toyo Utsunomiya-Shi, Tochigi 3218585, Japan

The amount of hydrogen gas generated is evaluated using a $G(H_2)$ value representing the amount of product generated per 100 eV when the substance absorbs energy, and a $G(H_2)$ value = 0.45 is given as an experimental value for hydrogen gas by the gamma-ray irradiation of water [4–15]. This value is the initial $G(H_2)$ value due to gamma-ray irradiation in pure water, and the pH dependence is considered to be small in past research. In order to more safely control the generation of hydrogen gas, various studies have been conducted on the setting of $G(H_2)$ value of hydrogen gas generated by radiolysis from waste. However, it has been reported that the value of $G(H_2)$ generated by radiolysis of water is also decreased by the presence of a scavenger of hydrogen precursor. For example, in an environment where nitrate exists, the amount of hydrogen generated by radiolysis of water is greatly reduced [16]. In this way, in order to apply it to actual waste, it is possible to evaluate the amount of hydrogen generated by radiation with higher accuracy by experimentally confirming the amount of hydrogen generated by radiolysis by irradiation tests simulating the environment around the target water.

In this study, gamma ray irradiation tests were conducted on ZMH contained in a Compacted Hull and End Piece waste generated from reprocessing facilities. In the irradiation test, the long-term catalytic effect on hydrogen generation G value was evaluated by gamma ray irradiation of water in the presence of a three-way catalyst, which is expected to suppress hydrogen generation. In a Compacted Hulls and End-Piece waste, ZMHcontaining adhered water (including bound water and unbound free water) and moisture adhering to the Compacted Hulls and End-Piece waste are cited as substances expected to generate hydrogen by radiolysis. In particular, ZMH has hygroscopic characteristics, so it is necessary to take into consideration the attached water [17–21].

A large amount of water (liquid water or steam) is assumed to degrade the catalytic function of the three-way catalyst used to recombine hydrogen. In addition, it has been reported that platinum (Pt), a main component of the three-way catalyst, is strongly poisoned by carbon monoxide (CO). Therefore, it is necessary to consider the deterioration of the catalytic function due to this poisoning [22, 23]. Therefore, in order to evaluate the hydrogen generation suppression effect of the poisoned three-way catalyst, a gamma ray irradiation test was carried out with an intelligent catalyst which is one of the three-way catalysts whose catalytic performance was confirmed. In addition, in order to evaluate quantitatively the reduction effect of hydrogen by catalyst by effectively arranging the catalyst, diffusion analysis simulation of hydrogen by natural convection in a Compacted Hulls and End-Piece waste was carried out.

Material and methods

Sample preparation

Preparation of ZMH simulated samples

In nuclear power generation, a large amount of fission products are generated by the fission reaction of uranium fuel, and spent fuel is generated. Spent fuel is dissolved in nitric acid in the reprocessing process to recover uranium and plutonium. As described above, ZMH adheres to the hull in the melting process, and moisture accompanies the Compacted Hulls and End-Piece waste by re-moisture absorption of ZMH. In order to evaluate hydrogen generation quantity by gamma-ray irradiation to ZMH contained in a Compacted Hulls and End-Piece waste, a sample was produced by simulating the generation process of ZMH in a reprocessing process. A ZMH simulated sample was prepared by dissolving a Mo compound and a Zr compound with Mo: Zr = 2: 1 using a 3 M aqueous nitric acid solution in the same manner as the solution in the reprocessing facility [24, 25]. The appearance of the prepared ZMH sample, SEM images, and XRD analysis results are shown in Fig. 1. It can be confirmed that $Zr(OH)_2Mo_2O_7(H_2O)_2$ powder has been prepared.

Pretreatment of irradiation test

The hull end pieces generated in the reprocessing facility will be filled in the compression container from the hull drum by a sorting and filling device, and nitrogen gas heated to 100 °C or higher will be ventilated inside the compression container for more than 1 h. After vacuum pumping and vacuum drying, it will be compressed by the compression device, filled in the waste container, and the lid will be welded and stored. Therefore, in the preparation of the irradiation specimen of the ZMH sample, the mixing of the ZMH sample, initial moisture absorption, drying, re-moisture absorption, and filling of the irradiation vessel were carried out as pretreatment in consideration of the planned processing step of the reprocessing facility. Specifically, the ZMH sample dried at 100 °C. for 1 h or more was stirred for about 10 min so as to have a uniform state, and the initial moisture absorption treatment was carried out so that the amount of moisture adhered to the ZMH sample was constant. As in the actual process at the reprocessing facility, the sample was dried at 100 °C. or more for 1 h or more, and then subjected to a re-moisture absorption treatment to be filled into the irradiation container.

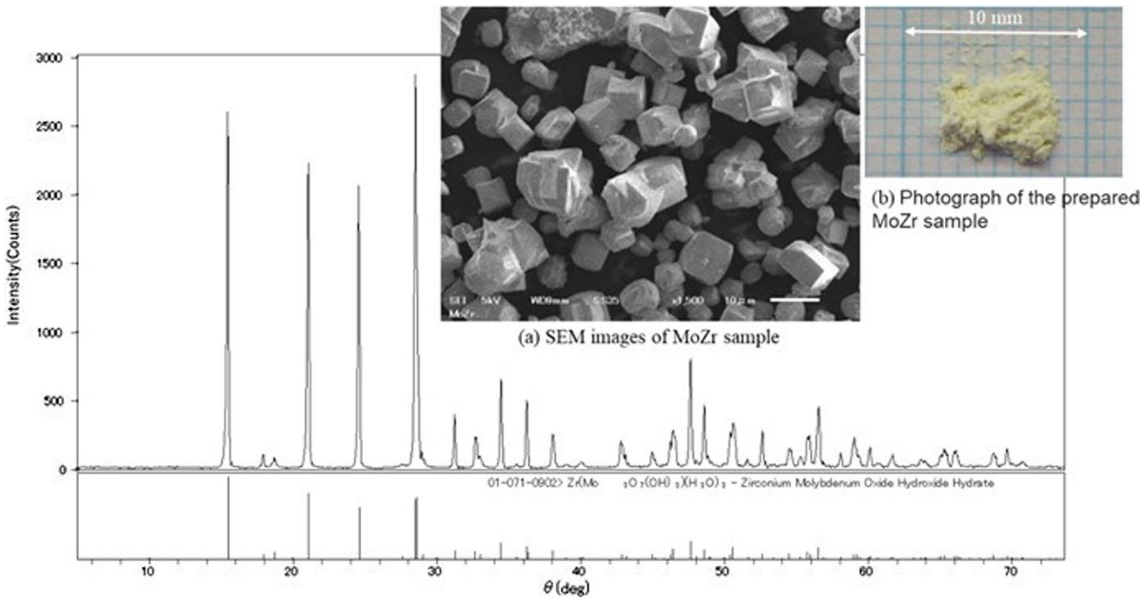

Fig. 1 XRD analysis results of ZMH sample **a** SEM images of ZMH sample, **b** Photograph of the prepared ZMH sample

Gamma irradiation test

Irradiation and post-irradiation tests

The irradiation of gamma rays was carried out in the Cobalt No. 1 Building No. 2 Irradiation Room of the Takasaki Institute for Quantum Applications, Atomic Beam Science Division, National Institute of Quantum Science and Technology, using Cobalt 60 as a radiation source. In order to meet the actual temperature conditions of the waste, two stainless steel thermostatic tanks resistant to gamma rays were installed in the gamma irradiation chamber. The temperature of the thermostatic chamber was controlled by a temperature controller and the heating temperature was monitored by calibrated thermocouples and data loggers. Since the compacts such as hulls have exothermic characteristics, irradiation tests were conducted at a dose rate of 8–11 kGy/h at 120 °C in consideration of the characteristics of zirconium molybdate.

In order to recover the gas generated by the gamma-ray irradiation test, the gas recovery equipment for recovering the gas immediately after the completion of irradiation was installed in the gamma-ray irradiation facility. The recovery system is a retrieval device for recovering the gas in the irradiation container after irradiation to the outside of the system by the pressure difference and to the recovery container. The hydrogen concentration in the irradiation vessel after irradiation was measured using a gas chromatograph (Thereafter, the gas chromatography). In this test, it was expected that the hydrogen concentration would differ greatly depending on the amount of generated hydrogen. Therefore, 2 sets of gas chromatography for low concentration measuring the hydrogen concentration of 5–50 ppm and medium and high concentration measuring the hydrogen concentration of 50–2,000 ppm were prepared. In order to measure the carbon monoxide concentration in the vacuum system, a Flame Ionization Detector (FID) with a methanizer was installed using a gas chromatograph detector for measuring the carbon monoxide concentration. The pressure and temperature at the time of measurement were recorded and converted into the concentration.

The G (H_2) value obtained by measuring the concentration of hydrogen generated in the vessel by irradiation was calculated and irradiation dose wase measured using aminogray. Here, the value is not based on the first order reaction of the radiolysis of water, but is a G (H_2) value indicating the final generation rate of hydrogen including the subsequent second order reaction of hydrogen and oxygen catalyzed recombination, and is thus distinguished as an effective G value. The weight of bound water was calculated from the weight returned by re-moisture absorption of the ZMH sample after drying (11.62% was the theoretical percentage of bound water due to re-moisture absorption of ZMH).

Long-term validation test of the catalyst under gamma irradiation

In this study, in order to investigate the effect of the presence of CO, NO_2 gas and steam, which may degrade the catalytic performance, on the reaction of the three-way catalyst, which is expected to be effective for suppressing the

increase of hydrogen concentration due to the radiolysis of water adhering to ZMH contained in Compacted Hulls and End-Piece waste, a gamma ray irradiation test was carried out in the presence of various poisoned gases. The catalyst weight was set at 0.4 g, and irradiation tests were carried out by adding 1 g of carbon graphite as a CO generation source and 1 g of excess water to the irradiation vessel in order to maintain the long-term coexistence of the poisoned gas. Since the added water is 1 g, most of the water exists in the liquid state even under the condition of heating at 120 °C., although a part of the water becomes steam (saturated steam amount: 0.084 g in 75 ml of the irradiation container). Although the catalyst is exposed to water vapor, it is not immersed in water. The water vapor content was calculated based on the equation of Teten.

The three-way catalyst used as the catalyst is a three-way catalyst developed as a catalyst for purifying automobile exhaust gas. By compounding Pt, Rh, and Pd as noble metal species with a honeycomb structure perovskite type oxide support material for increasing the surface area, the reduction in the surface area of the catalyst due to the growth of noble metal particles, which has been the cause of deterioration in the catalytic function, is highly suppressed, and the life of the catalyst function is extended [26–28]. In this reasearch, regarding a three-way catalyst (intelligent catalyst and CO poisoning resistant catalyst) which is expected to be effective for suppressing the increase of hydrogen concentration due to the radiolysis of water adhering to ZMH contained in hulls waste, a gamma-ray irradiation test was conducted in the presence of various poisoning gases in order to examine the effect of the presence of poisoning components such as CO and NO_2, which may cause the degradation of catalyst performance, on the reaction. The weight of each catalyst was 0.4 g. In the CO poisoning test, 7000 ppm CO concentration was added to the irradiation vessel, and the irradiation test was carried out by loading the intelligent catalyst or the CO poisoning resistant catalyst. In the NOx poisoning test, NO_2 concentrations of 20 ppm, 100 ppm, 1000 ppm and 5000 ppm were added to the irradiation vessel, and the NO_2 concentration in the irradiation vessel was used as a parameter, and the irradiation test was carried out by loading an intelligent catalyst or a CO poisoning resistant catalyst. In addition, when NO_2 and CO gas coexist, it is assumed that the oxygen concentration decreases due to the oxidation of NO_2 and CO gas. Therefore, assuming that the oxygen concentration decreases, an irradiation test was carried out by loading the irradiation vessel with nitrogen instead of air, taking the oxygen concentration as a parameter, and filling it with an intelligent catalyst or a CO poisoning resistant catalyst.

Hydrogen diffusion analysis simulation

In order to quantitatively evaluate the effect of the arrangement of the catalyst, flow analysis simulation by natural convection was carried out in a storage container of a Compacted Hulls and End-Piece waste, and flow analysis was carried out by dividing the flow passage in the storage container in which the Compacted Hulls and End-Piece waste is laminated and the upper space in which the catalyst is installed, and the convection inside the container and the catalyst installation effect were analytically evaluated using the open source code OpenFOAM.

Since the flow channel region in which hydrogen generated in a storage container in which a Compacted Hulls and End-Piece waste is laminated is very narrow, it is necessary to predict the flow of hydrogen in such a narrow channel. In this case, the hydrogen density is very small, and buoyancy generated by the density difference with the surrounding gas and driven by the density difference is indispensable to be considered. In this analysis, a natural convection analysis model was constructed for a narrow channel considering buoyancy due to density difference, and hydrogen concentration and velocity distribution released from the narrow part were predicted.

The flow analysis of the upper space was carried out in a two-dimensional axisymmetric manner using the flow analysis result of the narrow channel as a boundary condition. After that, the flow analysis of the upper space was carried out in three dimensions, and it was confirmed that there was no difference with the analysis result of two-dimensional axis symmetry. Based on these analysis results, we evaluated the catalytic effect and hydrogen diffusion behavior in the Compacted Hulls and End-Piece waste by the difference of the height (arrangement) of the catalyst.

The target flow analysis region was the upper space of a Compacted Hulls and End-Piece waste. Fig. 2 shows the schematic diagram of compacted hulls and end-piece waste and enlarged view of upper space of hulls container. For compacted hulls and end-piece waste, 6–7 compressors are enclosed in a stainless steel container, and air passages are secured at both ends of each compressor. The mesh of the three-way catalyst was 4×4 mm, and the outer shape was made to be a rectangular catalyst of 150×150 mm (simulated by a cylinder of equivalent diameter in two-dimensional axisymmetric analysis), and it was modeled by 2 kinds of porous body zone models of 25 and 50 mm in height, assuming a general-purpose product. The temperature conditions were set at 14 °C for both the upper space and the narrow space (the average of the maximum daily temperatures from 1981 to 2010 at the Mutsu Special Regional Meteorological Observatory), and were examined under conservative temperature conditions to reduce the diffusion of hydrogen at low temperatures.

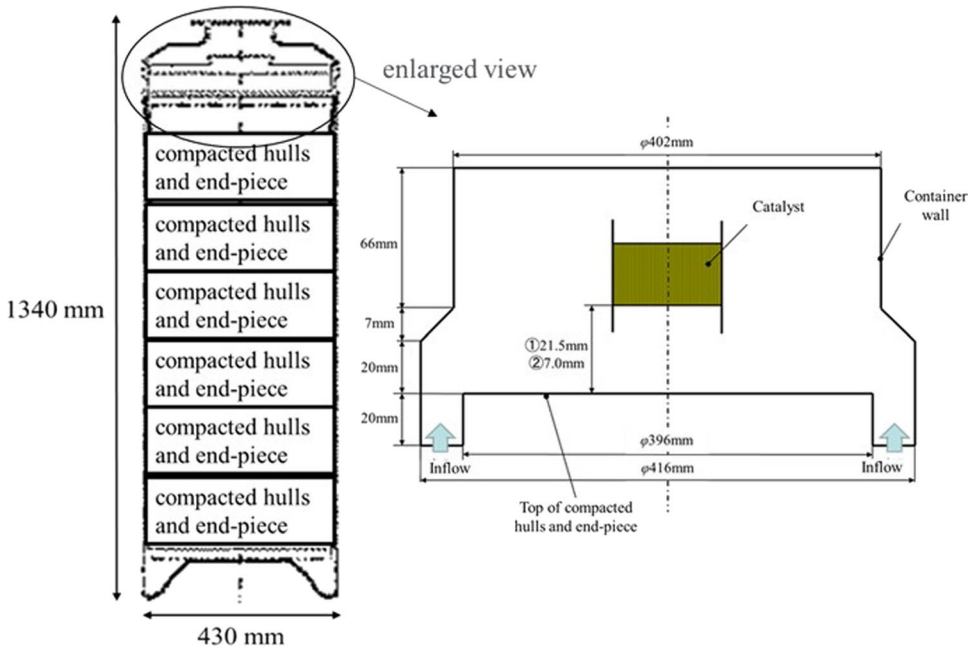

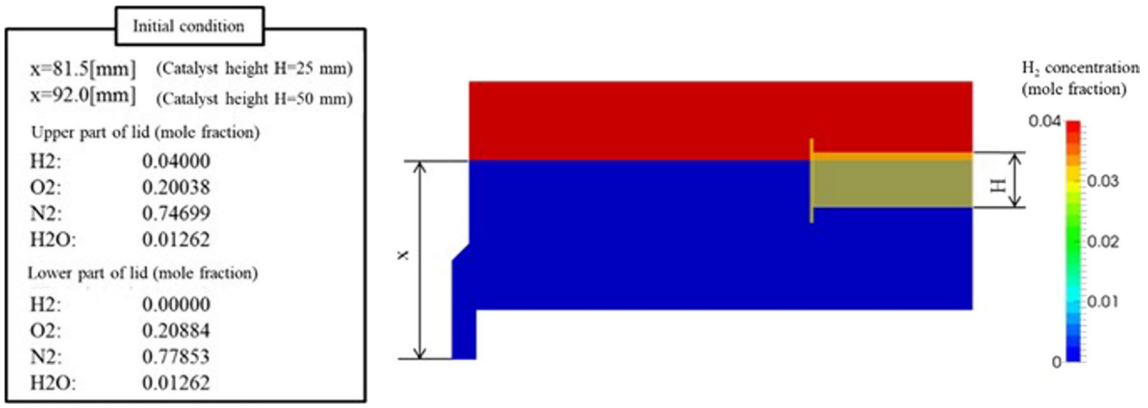

Fig. 2 Upper space and catalyst arrangement of compacted hulls and end-piece waste

Fig. 3 Hull canister upper model initial conditions (2D axisymmetric model)

Both the outer surface thermal conditions and the inner surface thermal conditions were insulated.

The inflow condition of gas (hydrogen flux and hydrogen concentration in the analysis of the narrow part) from the narrow part of the Compacted Hulls and End-Piece waste to the upper space was made to be a steady boundary condition. As a conservative initial condition, the analysis assumes that only the top (red portion of Fig. 3) is filled with 4% hydrogen. Others were filled with air. The parameters of the catalysts used in the analysis were those obtained through performance experiments in previous studies (Table 1) [29, 30]. Table 2 shows the analysis cases of the catalyst model. In addition to the two-dimensional analysis, the three-dimensional modeling of the upper space was performed to perform the analysis (Fig. 4).

Results

Gamma ray irradiation test of ZMH samples

Evaluation of long-term effectiveness of catalyst

Table 3 shows the results of gamma irradiation tests. In the irradiation test in which only water was added, the $G(H_2)$ value was 0.33, which was almost the same as the $G(H_2)$ value in the similar irradiation test system [31]. If the catalyst deteriorates under the present test conditions, the slope of the increase in hydrogen concentration relative to the cumulative dose may become steep due to the deterioration of the catalyst function. However, since the slope does not change significantly between 30 and 100 MGy, the degree of catalyst deterioration may be small.

Table 1 Catalyst parameters used in the analysis

Parameters	Value
Density	3890 kg/m^3
Specific heat	779 J/kgK
Thermal conductivity	36 W/mK
Mesh diameter	4 mm
Aperture ratio	0.735
Specific surface area	740 m^2/m^3
Frequency factor	450
Activation energy	5.751×10^6 J/kmol

In addition, since the hydrogen concentration increases linearly as shown in Fig. 5, it is considered that the formation of water molecules by the three-way catalyst is less than that of hydrogen molecules and oxygen molecules formed by the radiolysis of water and steam. Therefore, although oxygen is present and the catalyst is functioning, there is little change in the G value, indicating an increase in the hydrogen concentration. From the above results, it is considered that there is little degradation of the catalytic function of the three-way catalyst up to the cumulative dose of 100 MGy. The results of irradiation tests are shown in Table 4. CO concentration after gamma-ray irradiation was below the detection limit of 18 ppm in all catalysts, and it became clear that CO was oxidized to CO_2 by the catalyst. In addition, the effective G(H_2) value decreased as compared with the condition where CO did not coexist. No degradation of catalytic function due to CO poisoning was confirmed, and it was confirmed that the catalyst functioned sufficiently even in the presence of CO. With respect to the effective G(H_2) value, both the three-way catalyst and the CO poisoning resistant catalyst showed a similar tendency, and the effective G(H_2) value decreased as the NO_2 concentration increased, and the amount of hydrogen generated was suppressed more than that under the condition where the NO_2 concentration was zero. Consistent with the results, the results of the

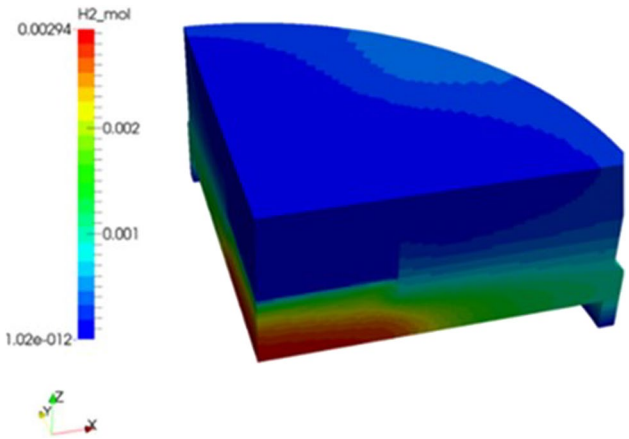

Fig. 4 Hull canister upper model 3D model

analysis after irradiation with NO_2 gas was much lower than the initial added NO_2 concentration. From the above results, it was not confirmed that the catalyst function deteriorated due to NO_2 poisoning, and it was confirmed that the catalyst functioned sufficiently even in the presence of NO_2. In the nitrogen atmosphere, it had been assumed that the recombination rate of hydrogen decreases because the concentration of oxygen decreases, but it became clear that the recombination of hydrogen proceeds even if the oxygen concentration is extremely decreased. In addition to the oxygen generated in the radiolysis of water, it is possible that adsorbed or oxidized substances on the catalyst surface are involved in the oxidation reaction.

Results of analysis of hydrogen diffusion

Analytical results of narrow parts inside compacted hulls and end-piece waste

Figure 6 shows the time-averaged velocity distribution and time-averaged concentration distribution. At this time, the time average is 138.9 h in real time. Figure 6 shows an

Table 2 Analysis case

		Catalyst shape		Initial condition		
		Mesh Diameter mm	Height mm	To the upper space hydrogen inflow condition	Temperature °C	Pressure Pa
Verification analysis of catalyst model (two-dimensional)	Case 1 -1	4	25	Calculated results of narrow part flow	14	101,325
	Case 1 -2	4	50	Calculated results of narrow part flow	14	101,325
Analysis of Hull Canister Upper Space (3D)	Case 2 -1	4	25	Calculated results of narrow part flow	14	101,325
	Case 2 -2	4	50	Calculated results of narrow part flow	14	101,325

Table 3 Effect of hydrogen generation g value in an air atmosphere at 120 °C

ZMH g	Catalyst g	Carbon graphite g	Added water g	Cumulative dose MGy	H_2 Generation μmol	$G(H_2)$ value
None	None	None	0.057	0.494	0.996	0.34
None	None	None	0.061	0.494	0.963	0.31
1.302	None	None	None	0.550	0.388	0.045
1.290	0.407	1.000	1.003	30.99	23.50	0.0063
1.303	0.402	1.006	1.004	30.99	26.06	0.0071
1.298	0.402	0.997	1.003	30.99	40.96	0.011
1.298	0.399	1.003	1.000	50.45	88.12	0.015
1.298	0.402	1.000	1.002	50.45	89.04	0.015
1.298	0.401	1.002	1.001	50.45	62.35	0.010
1.294	0.407	1.001	1.004	72.12	65.05	0.0075
1.293	0.404	1.001	1.000	72.12	76.75	0.0089
1.299	0.403	1.000	1.000	72.12	46.51	0.0054
1.295	0.401	1.014	1.005	102.5	116.3	0.0095
1.292	0.401	1.000	1.006	102.5	137.7	0.011
1.291	0.402	1.001	1.001	102.5	61.51	0.0050

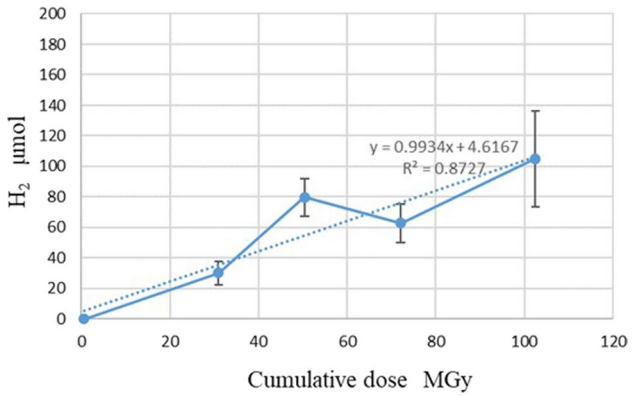

Fig. 5 Relationship between cumulative irradiation dose and hydrogen generation amount

enlarged view of the upper region of the hull or other compressible vessel. The time-averaged velocity is expressed as a dimensionless quantity divided by the emission velocity from the surface of the compression body such as the hull. The hydrogen concentration shows a value of $C \times 10^6$. Although the dimensionless velocity on the surface of the Compacted Hulls and End-Piece waste is 1, it can be understood from the analysis results that the accelerated flow is formed through the narrow gap. When the flow accelerated in the gap portion flows into the upper space region, the space region increases and the speed is rapidly decelerated.

The hydrogen concentration has a value of $C_W = 1.1 \times 10^{-6}$ on the surface of a Compacted Hulls and End-Piece waste, but in the region where the hydrogen concentration shifts from a small interval region in a narrow part to an upper space region, the hydrogen concentration has an order of 10^{-8}, indicating that the hydrogen concentration rapidly diffuses. It can be understood that the hydrogen concentration further decreases by one order of magnitude as the spatial region increases more than the narrow region when it reaches the upper spatial region. Table 5 shows the calculated values of the time average velocity and time average concentration at the outlet of the narrow part in a Compacted Hulls and End-Piece waste. The gap position shows a dimensionless value at a gap distance of 10 mm, where 0 represents the inner wall surface of a container containing a Compacted Hulls and End-Piece waste, and 1 represents the outer wall surface of the compressed hull. As described above, the velocity is a dimensionless value obtained by dividing by the rising velocity Uref = 10^{-6} m/s from the surface of the Compacted Hulls and End-Piece waste. The mainstream velocity of + indicates an upward flow,—indicates a downward flow, and the radial velocity of—indicates a velocity from the center toward the inner wall of the Compacted Hulls and End-Piece waste. The circumferential velocity has a value about two orders of magnitude lower than the velocity in the mainstream direction and the radial direction, and the value is almost zero. Since the hydrogen concentration is multiplied by the value of 10^6, the value of 1.1 is obtained at the gap position 1, that is, the wall surface of the Compacted Hulls and End-Piece waste. The hydrogen concentration in the vicinity of the inner wall side of the container containing the Compacted Hulls and End-Piece waste shows a value of $C = 2.26 \times 10^{-9}$, and it can be understood that the diffusion progresses rapidly even in the gap region.

Table 4 Hydrogen generation G value in catalyst poisoning of CO in gamma ray radiation environment at 120 °C

ZMH g	catalyst g	atmospheric gas	Cumulative dose MGy	CO concentration ppm	H_2 Generation µmol	$G(H_2)$ value
1.287	Intelligent Catalyst 0.41	CO 7000 ppm Air balance	0.698	18	0.033	0.0031
1.310	CO poisoning resistant catalyst 0.41	CO 7000 ppm Air balance	0.698	18	0.032	0.0029
1.295	Intelligent Catalyst 0.40	NO_2 20 ppm Air balance	0.698	–	0.034	0.0031
1.295	Intelligent Catalyst 0.40	NO_2 100 ppm Air balance	0.698	–	0.020	0.0018
1.299	Intelligent Catalyst 0.41	NO_2 1000 ppm Air balance	0.698	–	0.024	0.0021
1.306	Intelligent Catalyst 0.41	NO_2 5000 ppm Air balance	0.698	–	0.022	0.0019
1.306	CO poisoning resistant catalyst 0.41	NO_2 20 ppm Air balance	0.698	–	0.027	0.0024
1.309	CO poisoning resistant catalyst 0.41	NO_2 100 ppm Air balance	0.698	–	0.014	0.0013
1.292	CO poisoning resistant catalyst 0.40	NO_2 1000 ppm Air balance	0.698	–	0.018	0.0018
1.313	CO poisoning resistant catalyst 0.41	NO_2 5000 ppm Air balance	0.698	–	0.019	0.0017
1.292	Intelligent Catalyst 0.41	N_2	0.510	–	0.015	0.0019
1.308	CO poisoning resistant catalyst 0.41	N_2	0.510	–	0.0092	0.0012

Analysis of hydrogen diffusion in upper space (two-dimensional axisymmetric analysis)

Looking at the phenomenon in time series, hydrogen that initially accumulated in the upper part of the space reacts with the catalyst and the temperature rises, causing an upward flow from the catalyst, and the hydrogen concentration increases in the lower part of the space after 100 s. This is caused by the flow generated by the upward flow from the catalyst, and what has accumulated on the upper part has flowed. Under both conditions, when the time exceeds 500 s, most of the hydrogen in the space is consumed by the catalytic reaction, which weakens the circulating flow in the container, and hydrogen in the lower part of the space is mainly consumed by the catalyst carried by the combined flow of the circulating flow and the flow from the narrow part. As for the temperature distribution, OpenFOAM does not take into account the effect of heat dissipation to the catalyst, and as the heat of reaction is used to increase the temperature of the gas, the overall temperature is higher, but the temperature in the space gradually decreases due to the supply of low temperature gas from the narrow part.

As for the height of the catalyst, when comparing Fig. 7 with Fig. 8, in Fig. 7, the height of the catalyst is high, and the distance between the catalyst and the upper and lower wall surfaces is narrowed, so that the circulation of gas is deteriorated. On the other hand, in Fig. 8, since the height of the catalyst is low and the distance between the catalyst and the upper and lower walls is wide, it is considered that the gas circulates efficiently. According to the hydrogen concentration distribution, almost all of the hydrogen did not react after the gas passed from the lower part to the upper part of the catalyst, and it is considered that the hydrogen concentration rapidly decreased at the catalyst height of 25 mm where the gas circulated efficiently.

Analysis of hydrogen diffusion in the upper space (3D analysis)

Three-dimensional analysis was performed. The spatial distribution of hydrogen concentration at 100, 500, and 1000 s from the initial state for each analysis case is shown in Figs. 9 and 10. Figure 11 shows the transition of the mass of hydrogen in the upper space and the transition of the maximum concentration of hydrogen, respectively.

In comparison with the results of the two-dimensional axisymmetric analysis, although the secondary flow occurred in the horizontal section, the trends such as hydrogen concentration distribution in the vertical section were almost the same.

When the distribution at each analysis case and each time is compared with the two-dimensional axisymmetric

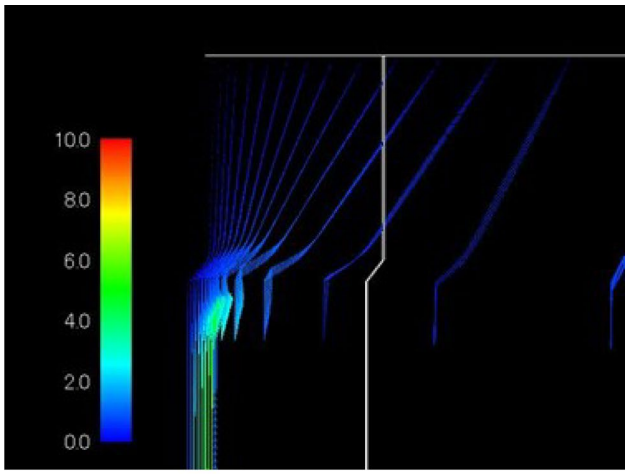

(a) Time average velocity

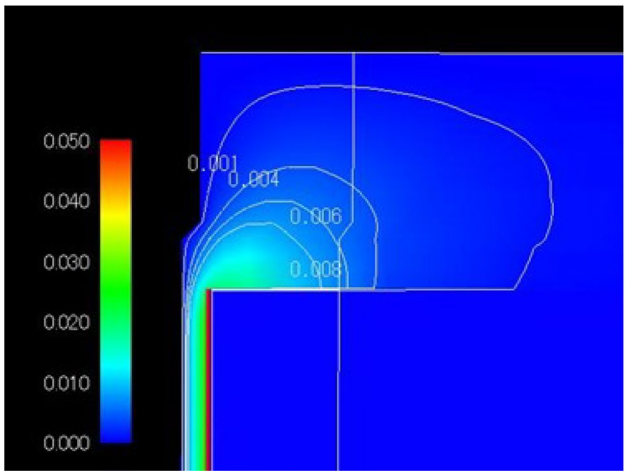

(b) Time average concentration (C x 10^6)

Fig. 6 Time average velocity distribution, time average concentration distribution of compacted hulls and end-piece waste

analysis result, it can be seen that the distribution in the circumferential direction occurs because the catalyst is rectangular. However, the distribution of the vertical cross section is almost the same as that of the two-dimensional axisymmetric analysis, and as a result, a circulating flow, i.e., an upward flow in the catalyst portion and a downward flow in the space side wall, is generated, and hydrogen in the vessel is gradually consumed by carrying hydrogen to the catalyst. The results of this analysis are different from those of the gamma irradiation test (initial hydrogen concentration: 0%) and the initial state (upper hydrogen concentration: 4% in the analysis). Therefore, the behavior of hydrogen concentration by the catalyst is different between this analysis result and the irradiation test.

With respect to the effect of the catalyst height, it can be seen that the smaller the catalyst height, the larger the gap with the container, and the stronger the circulating flow in the container. As can be seen from the transition of hydrogen quantity and the transition of maximum hydrogen concentration, the result is similar to the two-dimensional axisymmetric analysis result, and the lower the catalyst height, the more efficiently hydrogen is consumed. In addition, the results of two-dimensional axisymmetric analysis and three-dimensional analysis show good agreement quantitatively on the transition of these hydrogens, and it can be said that the effect of the rectangular shape of the catalyst on the cylindrical shape of the container is very small.

Analysis of hydrogen diffusion by generic analysis code (3D analysis)

Using the general-purpose thermal flow analysis code "ANSYS/Fluent" (Ver. 16.2), the authors carried out code-to-code verification with open source code and sensitivity analysis under the same flow analysis condition.

In case 2 -1,Fig. 12 indicated that indicated that hydrogen stratified in the upper part of the space at the initial stage infiltrates into the upper part of the catalyst part, and water vapor generated by the recombination reaction occurs there, causing convection in the upper part of the catalyst, and the water vapor and the infiltrated hydrogen form a small

Table 5 Time average velocity, time average concentration at the narrow outlet

Gap position	Circumferential velocity	Radial velocity	Mainstream directional velocity	H_2 concentration C × 10^6
0.00 E + 00	0.00 E + 00	0.00 E + 00	0.00 E + 00	0.00 E + 00
1.11 E − 01	− 1.55 E − 04	3.04 E − 02	3.46 E − 01	2.26 E − 03
2.22 E − 01	− 3.03 E − 04	7.59 E − 02	6.99 E − 01	4.52 E − 03
3.33 E − 01	− 4.45 E − 04	1.38 E − 01	1.06 E + 00	6.77 E − 03
4.44 E − 01	− 5.82 E − 04	2.21 E − 01	1.43 E + 00	8.98 E − 03
5.56 E − 01	− 7.15 E − 04	3.28 E − 01	1.80 E + 00	1.12 E − 02
6.67 E − 01	− 8.44 E − 04	4.71 E − 01	2.19 E + 00	1.33 E − 02
7.78 E − 01	− 9.70 E − 04	6.68 E − 01	2.58 E + 00	1.55 E − 02
8.89 E − 01	− 1.09 E − 03	9.56 E − 01	2.98 E + 00	1.76 E − 02
1.00 E + 00	0.00 E + 00	0.00 E + 00	1.00 E + 00	1.10 E + 00

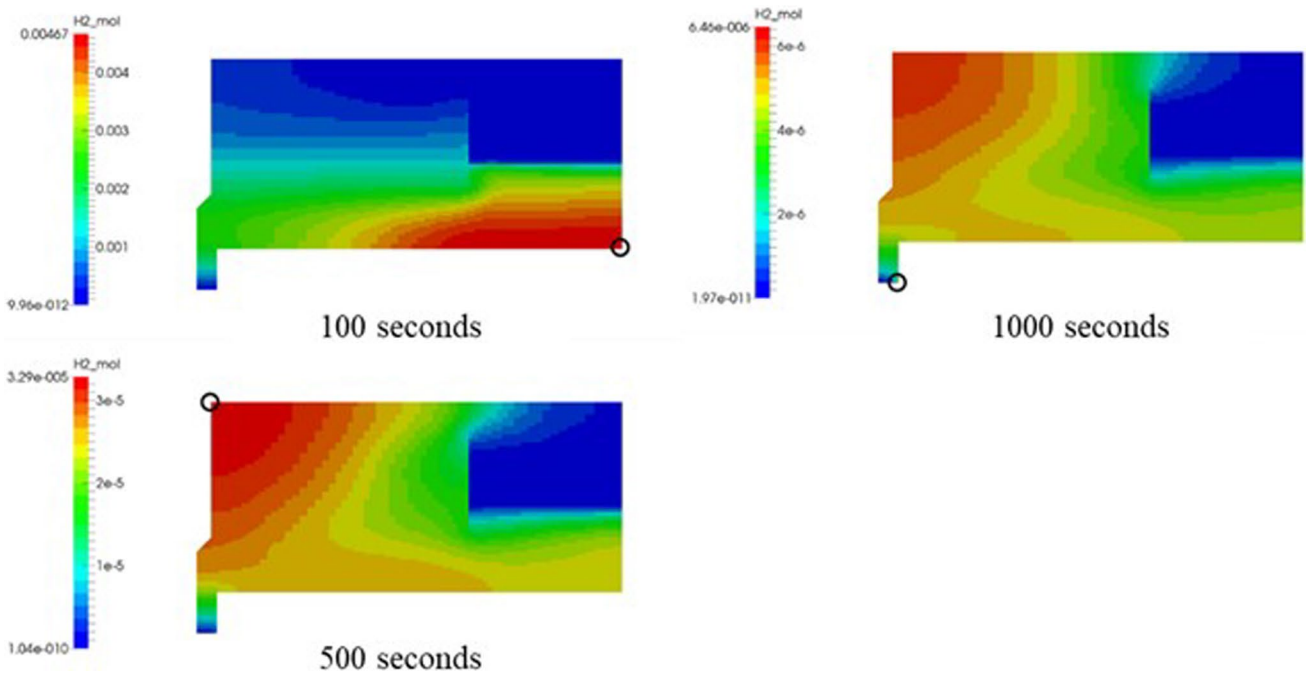

Fig. 7 Case 1 -1 (mesh diameter 4 mm, catalyst height 25 mm, hydrogen concentration (mole fraction))

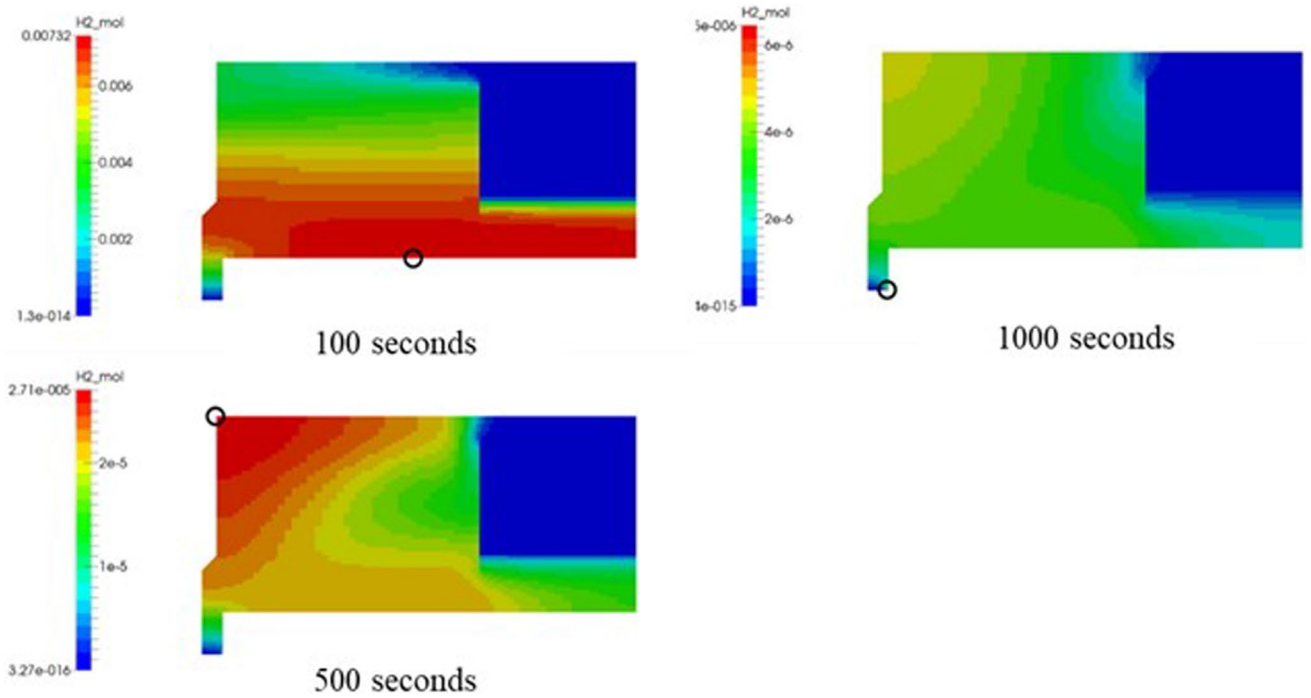

Fig. 8 Case 1 -2 (mesh diameter 4 mm, catalyst height 50 mm, hydrogen concentration (mole fraction))

circulating flow while mixing and diffusing. Over time, in the vicinity of the catalyst, a large circulating flow is formed over the entire upper space in such a manner that it branches into an ascending flow that bypasses the catalyst and an ascending flow that flows uniformly in the catalyst. The hydrogen treatment speed is high, and in the spatial distribution after 100 s, it is reduced below the flammability limit concentration. Further, as time passes, hydrogen

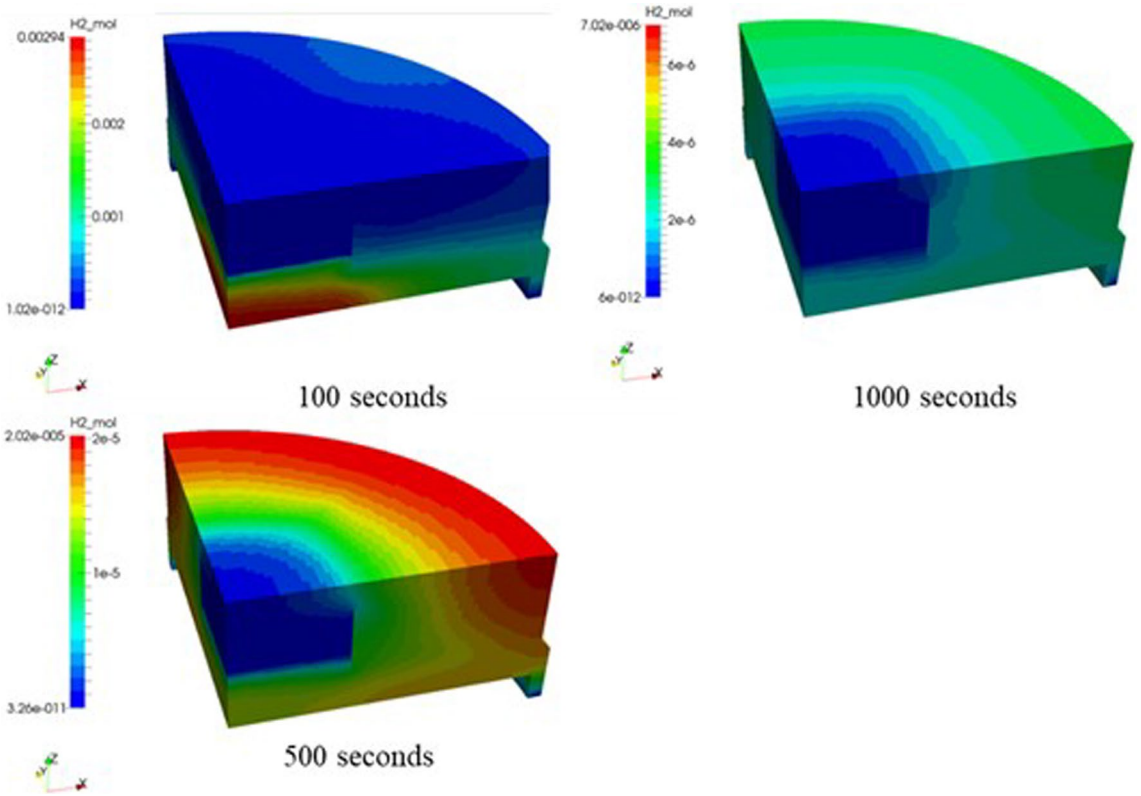

Fig. 9 Case 2 -1 (mesh diameter 4 mm, catalyst height 25 mm, hydrogen concentration (mole fraction))

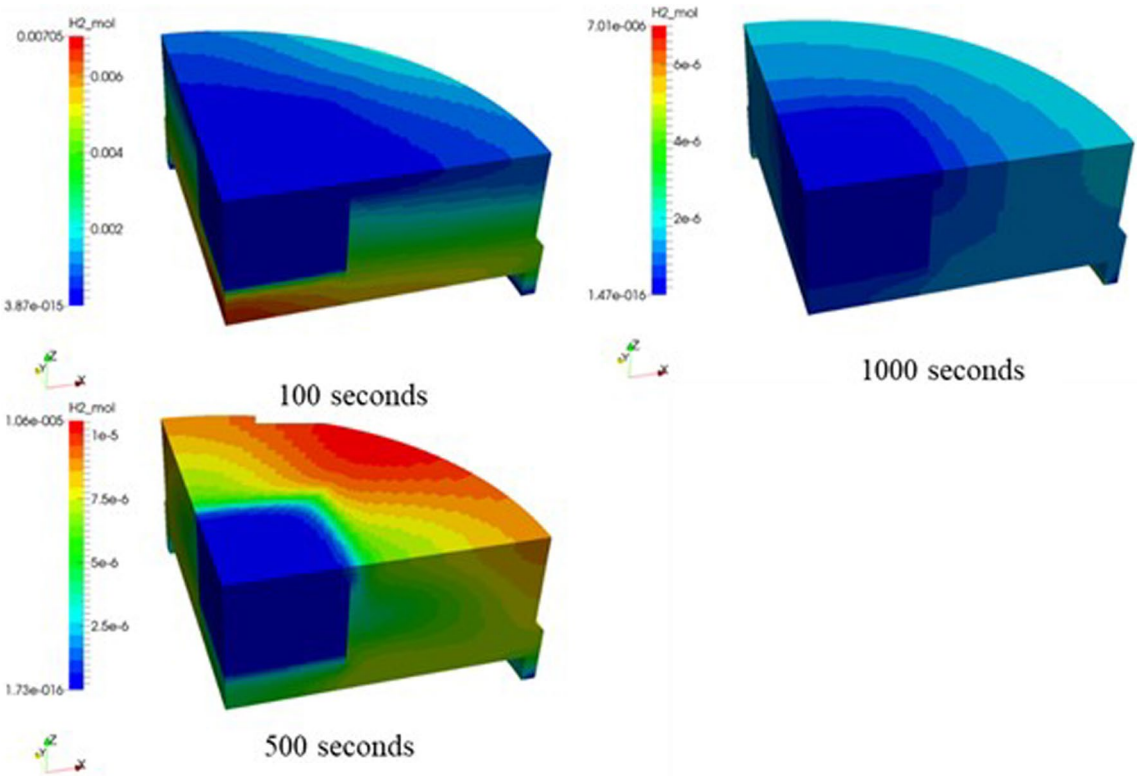

Fig. 10 Case 2 -2 (mesh diameter 4 mm, catalyst height 50 mm, hydrogen concentration (mole fraction))

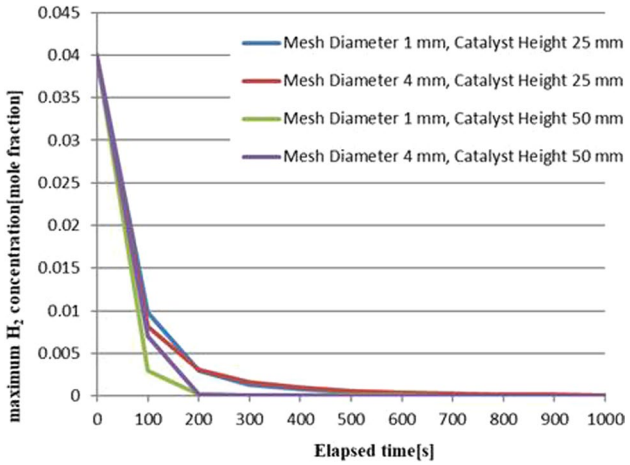

Fig. 11 Changes in the maximum concentration of hydrogen

generated by radiolysis in the compressor constantly flows in from the narrow part near the side wall, the narrow part becomes like a stagnant region against a large circulating flow forming the main stream in the upper space. Therefore, a slight concentration distribution is observed in the vicinity of the narrow part.

In case 2 -2,Fig. 13 showed that showed that due to the limitation of the installation conditions, the flow path of hydrogen stratified near the stainless steel inner lid and the upper part of the catalyst and steam subjected to the recombination reaction is narrowed, and the pressure loss of the catalyst part is increased, so that a small circulating flow in the upper part of the catalyst, which has been remarkably observed from the initial stage, is not observed, and a large circulating flow is formed in the upper space in such a manner that the catalyst is branched into a bypass flow and a flow that uniformly rises in the catalyst part. In the process in which the stratification of hydrogen collapses, it is considered that convection and diffusion of water vapor and hydrogen are induced by the recombination reaction at the upper part of the catalyst part as in case 2 -1. Since the reaction area is larger than that of the case 2 -1, the hydrogen treatment rate is reduced to the lower limit concentration of flammability or less in the spatial distribution after 100 s, as in the case 2 -1. The subsequent spatial distribution of hydrogen concentration is also similar to case 2 -1.

Fig. 14 displayed that the displayed that the hydrogen concentration distribution in the upper space is also common to each case, and the initial stratified interface collapses from the catalyst side, and the hydrogen concentration decreases because of rapid mixing diffusion and hydrogen recombination processing by the catalyst. In the upper space, hydrogen stagnation is formed in a part of the narrow part between the compressed body and the container wall, which is a boundary condition for steady hydrogen generation, due to circulating flow caused by mixed diffusion of hydrogen, steam, etc., and a gentle concentration gradient is observed at the starting point (maximum hydrogen concentration).

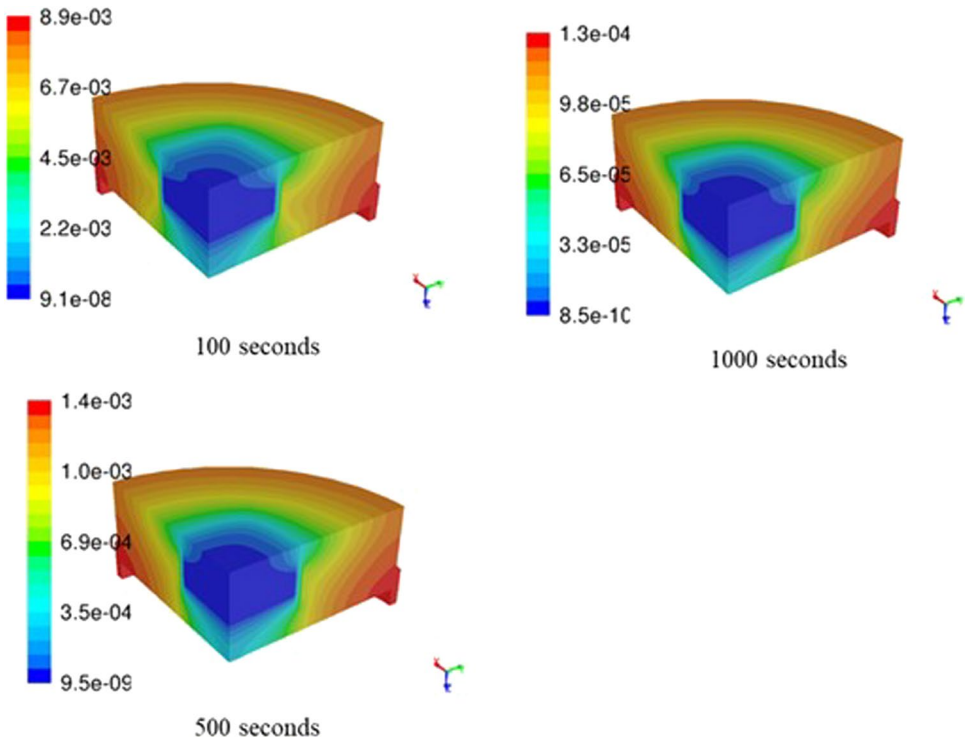

Fig. 12 Case 2 -1 (mesh diameter 4 mm, catalyst height 25 mm, hydrogen concentration (mole fraction))

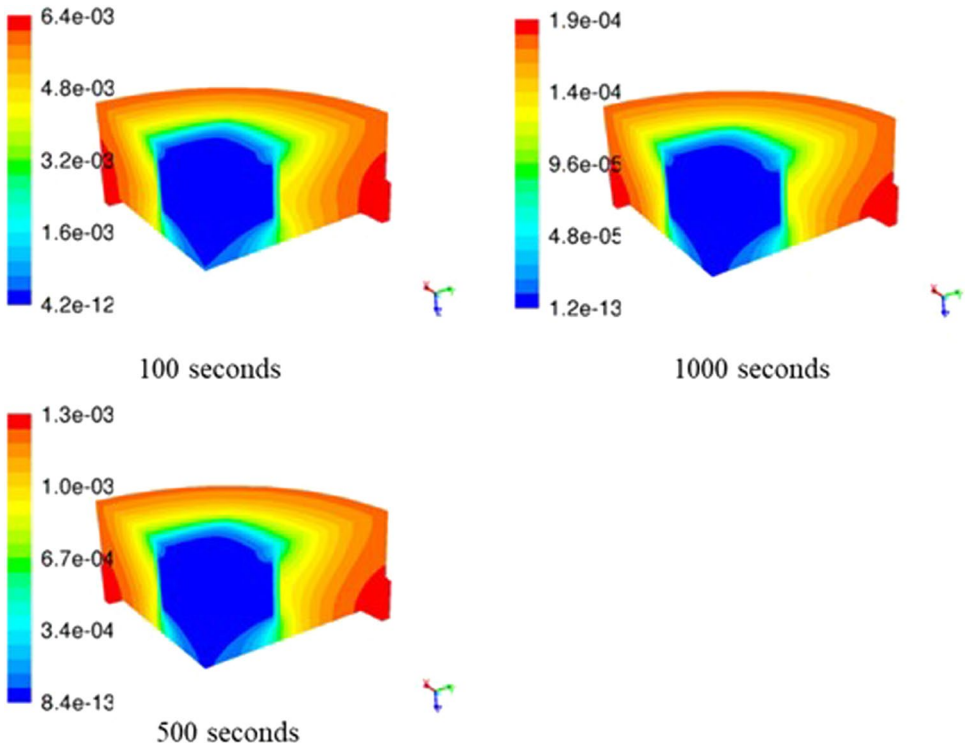

Fig. 13 Case 2 -2 (mesh diameter 4 mm, catalyst height 50 mm, hydrogen concentration (mole fraction))

The results of this analysis are different from those of the gamma irradiation test (initial hydrogen concentration: 0%) and the initial state (upper hydrogen concentration: 4% in the analysis). Therefore, the behavior of hydrogen concentration by the catalyst is different between this analysis result and the irradiation test.

Discussion

The OpenFOAM code, which is an open source code, and the ANSYS/FLUENT code, which is a general purpose code, were analyzed under the same conditions to cross-check the results. In the flow analysis in the narrow part, there was no significant difference in the hydrogen concentration distribution from the narrow part to the upper space by both codes.

For the catalyst model, the catalyst model of OpenFOAM resulted in too much catalytic reaction compared to the catalyst model of FLUENT. This is considered to be because the diffusion effect of gas in the passage space to the catalyst surface is not considered in the catalyst model of OpenFOAM. The frequency factor was multiplied by 1/130 in order to approximately reflect the diffusion effect in the analysis of OpenFOAM, and a good agreement was obtained with the analysis result of FLUENT. Therefore, in the analysis of hydrogen behavior and catalytic effects in the upper space, OpenFOAM can use a correction effect of 1/130 for the frequency factor.

In the flow analysis in the upper space (2D axisymmetric, 3D), quantitative analysis results for both OpenFOAM and FLUENT showed that hydrogen was rapidly consumed in the initial stage and tended to fall below the flammability limit concentration in both the two-dimensional and the three-dimensional analysis cases. In addition, within the range of this sensitivity analysis, it was confirmed that the reduction effect of pressure loss (when catalyst height is 25 mm and mesh diameter is 4 mm) was effective in promoting the hydrogen consumption rate.

In the long-term validation test of the three-way catalyst under gamma-ray irradiation, it was confirmed that the three-way catalyst functioned effectively without degradation of performance up to a cumulative dose of 100 MGy, which was the test condition. In addition, an irradiation test was conducted in consideration of the effects of CO, NO_2 and water vapor as poisoning gases that degrade the catalytic function, but no degradation of catalytic performance due to poisoning gases was observed under gamma irradiation. The cumulative dose of 1 MGy in an actual vessel corresponds to irradiation in about one year, but from the results of this study, the long-term effectiveness of the three-way catalyst was confirmed by using the catalyst.

Conclusions

In this study, the effect of the three-way catalyst on the hydrogen generation G value by the gamma ray irradiation of the water containing zirconium molybdate in the low level radioactive waste from the reprocessing plant was examined

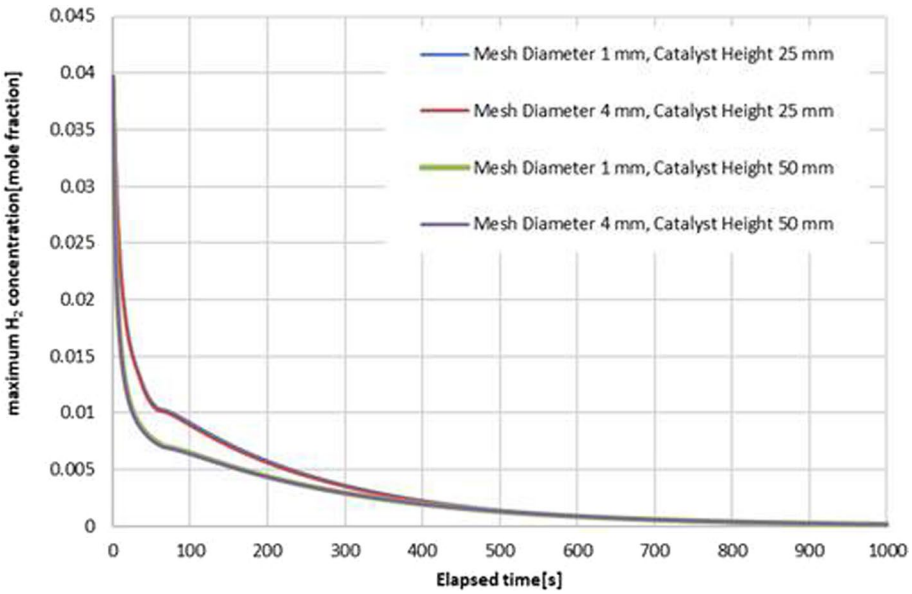

Fig. 14 Changes in maximum hydrogen concentration

experimentally. As a result of the irradiation test, the hydrogen generation $G(H_2)$ value under the non-catalyst condition showed a value on the order of 10^{-2}, while the effective $G(H_2)$ value considering the recombination reaction by the three-way catalyst showed a value on the order of 10^{-3}, which showed that the three-way catalyst was effective to suppress the hydrogen concentration increase by the radiolysis of water. When irradiation tests were conducted in the presence of poisoning gas (CO, NO_2 and water vapor), despite it may degrade the catalytic function, the effective $G(H_2)$ value was similarly as small as 10^{-3} orders of magnitude, and the results showed that the catalyst functioned sufficiently even in the presence of poisoning gas. Furthermore, it was confirmed that the performance of the three-way catalyst did not deteriorate up to a cumulative dose of 100 MGy, which is the test condition, and that the catalyst function was observed to be maintained to the level of cumulative doses.

Regarding the analysis of hydrogen diffusion, in the flow analysis using both the OpenFOAM and FLUENT codes, hydrogen was assessed to be rapidly consumed in the initial stage in all analysis cases, and the concentration tended to fall down below the flammable limit. The analysis results obtained show that the catalyst placement in the container of the Compacted Hulls and End-Piece waste can reduce the hydrogen concentration in the canister below the explosion limit by placing the catalyst at the center of the upper space considering the size limitation of general-purpose product, if the catalyst model and the catalyst placement in this study are used in practice.

From the above results, it is considered that hydrogen concentration can be suppressed even in long-term storage by utilizing a three-way catalyst which has the excellent characteristics of radiation resistance and poisoning resistance during the storage period of Compacted Hulls and End-Piece waste in Japan and has proved a long life of catalyst function.

Supplementary Information The online version contains supplementary material available at https://doi.org/10.1007/s10967-023-09251-2.

Acknowledgements We would like to thank Mr. Y. Katsumura for experimental design (The University of Tokyo). We also thank Mr. H. Noda and Y. Akinaga for information of compacted hulls and end pieces waste and for advice on experimental design (Japan Nuclear Fuel Limited). Finally, we are grateful to the referees for useful comments. The gamma-ray irradiation experiments were conducted at the Takasaki Advanced Radiation Research Institute, the National Institutes for Quantum Science and Technology (QST). A part of this work is supported by the Ministry of Economy, Trade and Industry (METI, Japan). The information presented in contribution is the sole opinion of the authors and does not necessarily reflect the views of the sponsoring.

Data availability The data that supports the findings of this study are available in this published article and its supplementary material.

Declarations

Conflict of interest The authors declare that they have no conflict of interest.

References

1. Hollis WK, Velarde K, Lashley J, Bustos L, Cournoyer M, Villarreal R (1998) Gas generation from contact of radioactive waste and brine. J Radioanal Nucl Chem 235(1–2):235–239
2. Atomic Energy Society of Japan Standard (2015) Manufacture requirements and inspection method for wastes subject to marginal depth disposal [in Japanese]
3. Japan Nuclear Fuel Limited, Reprocessing business designation application form for facilities, Attachment 8 [in Japanese]
4. Draganic I (1971) The radiation chemistry of water. Academic Press
5. Bjergbakke E, Sehested K, Lang Rasmussen O, Christensen H (1984) Input Files for Computer Simulation of Water Radiolysis, Roskilde: Danmarks Tekniske Universitet, Risø Nationallaboratoriet for Bæredygtig Energi. Risoe-M, No. 2430
6. Ruiz CP, Lin CC, Robinson RN, Burns WG, Curtis AR (1989) Model calculations of water radiolysis in BWR primary coolant. Water Chem Nuclear Reactor Syst 5(2):131
7. Buxton GV, Elliott AJ (1991) High temperature water radiolysis and its relevance to reactor coolant, In: Proceedings 1991 JAIF international conference on water chemistry and nuclear power plants, Fukui City, pp. 283-288
8. Kent MC, Sims HE (1992) The yield of γ-radiolysis products from water at temperatures up to 300 °C, Water Chemistry of Nuclear Reactor Systems 6, BNES 1992 and AEA-RS -2302, Harwell
9. Elliot AJ, Oullette DC, McClacken DR (1992) High-temperature pulse radiolysis facility, AECL -10667. Atomic Energy of Canada Ltd., Canada
10. Elliot AJ, Chenier MP, Ouellete DC (1993) Temperature of g-values for H_2O and D_2O radiated with low energy transfer radiation. J Chem Soc, Faraday Trans 89:1193–1197
11. LaVerne JA, Pimblott SM (1993) Diffusion-kinetic modeling of the electron radiolysis of water at elevated temperatures. J Phys Chem 97:3291–3297
12. Sunaryo GR, Katsumura Y, Shirai I, Hiroishi D, Ishigure K (1994) Radiolysis of water at elevated temperatures-I, Irradiation with gamma-rays and fast neutrons at room temperature. Radiat Phys Chem 44:273–280
13. Elliott AJ (1994) Rate constants and g-values for the simulation of the radiolysis of light water over the range 0–300 °C, AECL Report AECL -11073
14. Christensen HC (2006) Fundamental Aspects of water coolant radiolysis, SKI Report
15. LaVerne JA (2004) Radiation chemical effects of heavy ions. In: Mozumder A, Hatano Y, Dekker M (eds) Charged particle and photon interactions with matter. CRC Press, New York
16. Pastina B, LaVerne JA, Pimblott SM (1999) Dependence of molecular hydrogen formation in water on scavengers of the precursor to the hydrated electron. J Phys Chem A 103(29):5841–5846
17. Zhang L et al (2013) Evaluation of precedence behavior of zirconium molybdate hydrate. Front Chem Sci Eng 7(1):65–71
18. Stevens R, Linford J, Woodfield BF, Boerio-Goates J, Lind C, Wilkinson AP (2003) Heat capacities, third-law entropy and thermodynamic functions of the negative thermal expansion materials, cubic α-ZrW2O8 and cubic ZrMo2O8, from T = (0 to 400) K. J Chem Thermodyn 35:919–937
19. Douucet FJ et al (2002) The formation of hydrated zirconium mo1ybdate in simulated spent nuclear fuel reprocessing solutions. Phys Chem Chem Phys 4:3491–3499
20. Usami T et al (2010) Formation of zirconium polybdate sludge from a radiated fuel and its resolution into mixture of nitric acid and hydrogen peroxide. J Nucl Mater 402:130–135
21. Rao BSM et al (1990) Characterization of the solids formed from simulated nuclear fuel reprocessing solutions. J Nucl Mater 170(39):49
22. Watanabe M, Uchida H (2001) Shingata Denchi no Zairyo Kagaku, (Eds.) by The Chemical Society of Japan, pp. 167–195
23. Ralph TR, Longarth MP (2002) Platinum Metals Review 46: 117135. 52
24. Lind C, Wilkinson AP, Rawnb CJ, Andrew Payzant E (2001) Preparation of 'the negative thermal expansion material cubic ZrMo 2 O 8. J Mater Chem 12:3354–3359
25. Rao BSM et al. (1986) Solids formation from synthetic fuel reprocessing solutions: characterization of Zirconium Molybdate by ICP, XRF, and Raman Microprobe Spectroscopy
26. Nishihata Y, Mizuki J, Akao T, Tanaka H, Uenishi M, Kimura M, Okamoto T, Hamada N (2002) Self-regeneration of a Pd-perovskite catalyst for automatic emissions control. Nature 418:164–167
27. Tanaka H, Uenishi M, Taniguchi M, Tan I, Narita K, Kimura M, Kaneko K, Nishihata Y, Mizuki J (2006) The intelligent catalyst having the self-regenerative function of Pd, Rh and Pt for automatic emissions control. Catal Today 117:321–328
28. Hirata S, Mouri T, Igarashi M, Satoh M, Kamiji Y, Nishihata Y, Taniguchi M, Tanaka H, Hino R (2015) Development of new type passive autocatalytic recombinant—Part 2 proposal of conceptual structure. E-J Adv Maint, Japan Soc Maint 7(1):122–128
29. Agency of Natural Resources and Energy (2014) "Project for Improvement of Technology Infrastructure for Nuclear Power Reactor Safety Measures (Improvement of Hydrogen Safety Technology)"
30. Agency of Natural Resources and Energy (2016) "Project for Improvement of Technology Infrastructure for Nuclear Power Reactor Safety Measures (Improvement of Hydrogen Safety Technology)"
31. Elliot AJ, Chenier MP, Ouellette DC (1990) g-Values for y-radiated water as a function of temperature. J Chem 68:712